

Vacuum Bubble in an Inhomogeneous Cosmology: A Toy Model

W. Fischler, S. Paban, M. Žanić

Department of Physics

University of Texas

1 University Station, C1608

Austin, TX 78712

E-mail: fischler@physics.utexas.edu, paban@physics.utexas.edu,
marija@mail.utexas.edu

C. Krishnan

International Solvay Institutes

Physique Théorique et Mathématique

ULB C.P. 231, Université Libre de Bruxelles,

B-1050, Bruxelles, Belgium

E-mail: Chethan.Krishnan@ulb.ac.be

ABSTRACT: We study the propagation of bubbles of new vacuum in an inhomogeneous generalized Lemaître-Tolman-Bondi background that includes a cosmological constant. This exemplifies the classical evolution of a tunneling bubble through a metastable state with curvature inhomogeneities, and will be relevant in the context of the Landscape. For the inhomogeneity profiles that we analyzed, we find that in terms of the invariant coordinates on the bubble (and in terms of the inside coordinates), the evolution is qualitatively similar to that of vacuum bubble propagation on a de Sitter background. Our setup should also be a useful toy model for capturing the effects of ambient inhomogeneities on an inflating region.

KEYWORDS: .

Contents

1. Introduction	1
2. Setup: The Bubble and the Background	3
3. Bubble Expansion in a Homogeneous Background	5
3.1 Homogeneous Background without Matter	6
3.2 Homogeneous Background with Matter	11
3.2.1 $R > R_{cr}$	13
3.2.2 $R < R_{cr}$	14
4. Bubble Expansion in Inhomogeneous Background	15
4.1 Generating a Curvature Profile	15
4.2 Examples	16
5. Conclusions	19
6. Acknowledgments	23
7. Appendix	23

1. Introduction

Although bubble propagation in homogeneous cosmological backgrounds has been amply studied [1]-[3], bubble propagation in inhomogeneous backgrounds is virtually unexplored [4]. Since tunneling is of enormous importance [5, 6] in populating the string Landscape [7, 8], we expect that the evolution of a new Universe through an old one, is worthy of study.

One reason for the lack of emphasis on inhomogeneous backgrounds is the cosmic no-hair theorem [9, 10]. This theorem states that the evolution of an expanding universe that contains a cosmological constant will eventually be dominated by vacuum energy, and will asymptote to a de Sitter space. It will imply in particular, that inhomogeneous backgrounds containing a cosmological constant (like the ones constructed on Landscape vacua) will evolve toward ‘ironing out’ such inhomogeneities, and therefore it will make sense to restrict the study of bubble propagation to homogeneous backgrounds. But to the best of our knowledge, the cosmic no hair theorem has not been unambiguously proven, nor have its hypotheses been clearly stated, thus warranting a re-appraisal of the problem.

One particular work that stands out in this context is that of Wald [11], who did a comprehensive study of the late time evolution of anisotropic but homogeneous spaces with a cosmological constant. In this restricted setting, he was able to define the conditions for the cosmic no hair theorem to be satisfied by taking advantage of the Bianchi classification of homogeneous, anisotropic metrics. Wald studied the time evolution of such metrics when the energy momentum tensor is the sum of two components: a cosmological constant and a term that satisfies the dominant and strong energy conditions. He found that with the exception of the Bianchi IX, the other models will always asymptote to a de Sitter space, within a time scale $\sqrt{\frac{3}{\Lambda}}$. In the case of the Bianchi IX models, the future behavior depends on the relative sizes of the cosmological constant and the spatial-curvature. Only when the latter exceeds the cosmological constant will the time evolution *not* be asymptotically de Sitter.

It is often claimed that inflation solves the horizon and flatness problems but, as already remarked in its early years, these claims are based on the assumption that the pre-inflationary state of the universe can be described by a homogeneous and isotropic Friedmann-Robertson-Walker (FRW) space. Under these strong assumptions, inflation does indeed reduce considerably the amount of fine tuning necessary to explain the current experimental measurements. In general, however, one expects a high degree of inhomogeneity in the initial conditions, with some regions of the universe expanding while others contract. Holographic cosmology might be the only exception to this rule because it naturally produces a homogeneous and almost flat space-time [12, 13, 14].

The question of whether an inflating region can continue to inflate if the ambient region is inhomogeneous, has been explored by several authors for different pre-inflationary backgrounds. In a set of papers [16, 15, 17], Goldwirth and Piran sought to answer the question of whether large inhomogeneity in the very early universe could prevent it from entering a period of inflation. In their work, inflation was not driven by a cosmological constant but by an inflaton field. Their analysis is numerical and restricted to an inhomogeneous but isotropic and closed-universe background. They found that a large initial inhomogeneity could indeed suppress the onset of inflation, and that the inflaton field must have a suitable value over a region of several horizon sizes in order for inflation to start. This last finding raises the issue of an acausal initial condition. Other numerical simulations disagree with these results claiming that inhomogeneous backgrounds will have enough inflation to explain current observations [24, 25]. Analytical computations that use the long wave-length approximation seem to confirm that large inhomogeneities of the spatial curvature prevent the onset of inflation [18, 19, 20].

In this work, we will not be able to conclusively settle this issue once and for all. Instead, our goal here is to study a particular problem that we believe captures some of the same physics by playing local curvature effects against the might of the cosmological constant. The problem we consider is the classical evolution of a vacuum bubble in an inhomogeneous background, containing a cosmological constant and dust. This background, which we will

refer to as the Lemaître-Tolman-Bondi (LTB) space-time ¹, will be the simplest possible inhomogeneous space, spherically symmetric and with only one center [21]-[23]. The bubble will be created in a region of space that is expanding but will encounter through its evolution regions of varying curvature. In a nutshell, the problem is that the critical size for bubble nucleation depends locally on the scale factor. As this factor changes as a function of the position of the shell, it is possible for a supercritical bubble to become subcritical ². Our analysis will be confined to the evolution of the bubble, it will not address the interesting issue of tunneling probabilities in inhomogeneous backgrounds. This latter issue is very complicated, some attempts to address it have been made in [26].

In the next section we shall describe the LTB model that represents the background on which the bubbles will propagate. In section 3, we will review the propagation of bubbles in a homogeneous background. We will consider the already known case where the outside background is simply a de Sitter space, either flat or closed, and the novel case where matter is added to the cosmological constant. In this latter case, we shall explore the interesting situation of a bubble moving in a background that evolves from expanding to collapsing. In section 4 we shall study the truly inhomogeneous LTB background. We have relegated to the Appendix, an explanation of the known formalism to study the propagation of bubbles in general relativity.

2. Setup: The Bubble and the Background

A propagating bubble divides the space-time into three regions: outside, shell and inside. To give a proper description of this space-time in general relativity we will make use of the junction conditions, first presented by Israel [1] and extensively used since then by many authors. In particular, we will follow the implementation of this formalism developed by Berezin, Kuzmin and Tkachev [2].

The model we will study consists of a bubble of true vacuum propagating on a metastable state whose energy-momentum tensor contains a higher cosmological constant and dust. In addition, we will assume that this outer space-time is asymptotically flat. The bubble is assumed to be a thin-shell, with a perfect-fluid energy-momentum tensor whose equation of state will be allowed to vary. The true vacuum will be assumed homogeneous and isotropic while the outside background will be assumed to be spherically symmetric about one point in space. The line element of the outside region [27] is:

$$ds^2 = dt^2 - \frac{[a(t, r) + ra'(t, r)]^2}{1 - \frac{r^2}{R^2(r)}} dr^2 - a^2(t, r) r^2 d\Omega_2 \quad (2.1)$$

The expansion parameter $a(t, r)$ is both a function of time and of the radial coordinate r . Partial derivatives with respect to the radial coordinate will be represented by a prime. The

¹We slightly generalize it from the original form to allow for a positive cosmological constant.

²A bubble that can become subcritical in the future is a fluctuation, not a phase transition.

function $R(r)$ is an arbitrary function of the radial coordinate only and will be taken to be positive everywhere. We will study the evolution of the bubble for different choices of $R(r)$. It can be seen from these equations that we can choose a function $R(r)$ and then integrate for $a(t, r)$ at each r . Then we can use this $a(t, r)$ to *define* the $d(t, r)$ in (2.4), with the caveat that the choice of $R(r)$ has to be made in such a way that this energy density needs to be positive. Therefore, the description of the spacetime is essentially complete (apart from fixing certain initial conditions which we will get to in a minute), once we specify the function $R(r)$. Because it is our prejudice that curvature will interfere with the expansion of the bubble, when its value is comparable to the cosmological constant, we will choose $R(r)$ such that the curvature tends to zero for large radii but for small radii can overwhelm the effect of the cosmological constant.

The equations of motion for the expansion factor and the dust density $d(t, r)$, in units where $8\pi G = c = 1$, are:

$$\left(\frac{\partial_t a(t, r)}{a(t, r)}\right)^2 + \frac{1}{a^2(t, r)R^2(r)} = \frac{A}{a^3(t, r)} + \frac{\Lambda_{out}}{3} \quad (2.2)$$

$$\frac{1}{3}d(t, r)a^2(t, r)(a(t, r) + ra'(t, r)) = A \quad (2.3)$$

A is a constant. These equations reduce to the familiar Friedmann-Robertson-Walker equations in the limit where $R(r)$ is independent of the radial coordinate. Besides choosing $R(r)$ the solution to the equations of motion will involve the choice of the initial condition $a(t_0, r)$. For simplicity, we will choose this function to be independent of the radial coordinate r .

The results that will be presented in the forthcoming sections correspond to different choices of the function $R(r)$. For different choices of $R(r)$, the collapse-profile can be completely different. One way to understand this is to notice that the Friedmann-type equation here can be thought of as an energy equation for a particle of zero total energy in a potential

$$V(a) = -\frac{A}{a} - \frac{\Lambda_{out}a^2}{3} + \frac{1}{R^2} \quad (2.4)$$

For those values of r for which the maximum of this potential is above zero, if the universe starts at a big-bang, it will recollapse, but for other values of r there is no recollapse.

The bubble will be assumed to be a thin-shell (described by a hypersurface Σ) and spherically symmetric. Its energy momentum tensor will be assumed to be of a perfect-fluid type: $S_\tau^\tau = \sigma, S_\theta^\theta = S_\phi^\phi = -P, P = w\sigma$ and with the metric:

$$ds^2|_\Sigma = d\tau^2 - \rho^2(\tau)d\Omega_2 \quad (2.5)$$

The interior of the bubble will be assumed homogeneous and described by

$$ds^2 = dT^2 - b^2(T) \left(\frac{dz^2}{1+z^2} + z^2 d\Omega_2 \right) \quad (2.6)$$

with the following equation of motion for the scale factor:

$$\left(\frac{db}{dT}\right)^2 = \left(\frac{\Lambda_{in}}{3}\right)b^2(T) + 1 \quad (2.7)$$

We are assuming the inner space-time of the bubble to be open as derived from a tunneling process [28].

Given this setup, our aim is to understand the evolution of the bubble. The dynamics of the bubble is governed by the Israel junction conditions, the details of which are relegated to an appendix. The coupled differential equations that govern shell evolution turn out to be (7.8), (7.10), or in a more explicit form, (7.22), (7.24).

As always in general relativity, along with the dynamical equations, we also need an equation of state to fully specify the dynamics. Determining the equation of state between σ and P on the shell from first principles is a difficult problem that requires a field theoretic model for matter on either side. Since the LTB metric for a generic choice of the curvature profile $R(r)$ is known only numerically, this is doomed from the start. In the absence of a detailed understanding of this phase transition we will confine our study to perfect-fluid shells, $P = w \sigma$, and explore various values of w .

It turns out that in the absence of dust on the outside, the shell-evolution equations can be written entirely in terms of $\rho(\tau)$ because (7.10) becomes trivial, but this is no longer possible when dust is included. Indeed, equation (7.8) can be written as (reproduced from the appendix):

$$\dot{\rho}^2 = -1 + B^2 \rho^2, \quad (2.8)$$

$$B^2 = \frac{\Lambda_{in}}{3} + \left(\frac{\sigma}{4} + \frac{1}{\sigma} \left(\frac{\Lambda_{out} - \Lambda_{in}}{3} + \frac{A}{a^3}\right)\right)^2. \quad (2.9)$$

In general, to fix the evolution of $B(\tau)$ we need (7.10), along with a knowledge of the scale factor through numerical solution of (2.2).

We also get constraints on the parameters and the allowed phase space from the positivity of energy, in particular, the condition that σ be positive. The explicit relations that we will use later can again be found in the appendix.

3. Bubble Expansion in a Homogeneous Background

The study of the bubble evolution can be done in different sets of coordinates. When dust is present, the problem of interest is most conveniently analyzed in the coordinates of the outside background. To familiarize ourselves with these coordinates we will devote this section to analyze a simpler problem. The simplification will come from restricting the outside background to be homogenous ($R(r) = \text{constant}$). First, we will redo the well studied motion of a vacuum shell in a cosmological constant background. Then we will add a dust energy density to the cosmological constant.

3.1 Homogeneous Background without Matter

The Israel junction conditions (7.8)-(7.10) tell us that it is consistent to have a vacuum shell (surface energy is constant and $w = -1$) in a transition that separates two de Sitter spaces with different values of the cosmological constant. Since this problem has been solved many times in the literature we will only quote the results [2] .

In terms of the intrinsic bubble coordinates, the motion of the shell is given by:

$$\rho(\tau) = \frac{1}{B} \cosh B\tau$$

where

$$B^2 = \frac{\Lambda_{in}}{3} + \left(\frac{\sigma}{4} + \frac{\Lambda_{out} - \Lambda_{in}}{3\sigma} \right)^2$$

regardless of the curvature of the outside background. The effect of this curvature only becomes manifest when we express the motion of the bubble in terms of the outside coordinates. In these coordinates the evolution of the position of the bubble is given by:

$$\frac{dx}{dt} = \frac{-(1 - \frac{x^2}{R^2}) \sqrt{(\frac{\Lambda}{3} - \frac{1}{a^2 R^2})} \pm \sqrt{(B^2 a^2 x^2 - 1)(B^2 - \frac{\Lambda}{3})(1 - \frac{x^2}{R^2})}}{a^2 x (B^2 - \frac{1}{a^2 R^2})} \quad (3.1)$$

where the further assumption that $\Lambda_{in} = 0$ and $\Lambda_{out} = \Lambda$ has been made. The evolution of the scale factor is given by the well known expression

$$\left(\frac{da/dt}{a} \right)^2 + \frac{1}{a^2 R^2} = \frac{\Lambda}{3}$$

For times $t \gg \frac{1}{H} = \sqrt{3/\Lambda}$, (3.1) reveals the following asymptotic behavior :

$$a(t) \rightarrow \frac{1}{2HR} e^{Ht} \quad \text{when} \quad a(0) = \frac{1}{HR} \quad (3.2)$$

$$x(t) \rightarrow R \sin \left(\frac{\text{constant}}{R} \right) - O(e^{-Ht}) \quad \text{if } R > 0 \text{ and finite} \quad (3.3)$$

$$x(t) \rightarrow \text{constant} + O(e^{-Ht}) \quad \text{if } R \rightarrow \infty \quad (3.4)$$

$$\frac{dx}{dt} \rightarrow \frac{1}{a} \sqrt{1 - \frac{x^2}{R^2}} \frac{\frac{\sigma}{4} - \frac{\Lambda}{3\sigma}}{\frac{\sigma}{4} + \frac{\Lambda}{3\sigma}} \quad (3.5)$$

The value of the constants in (3.3) and (3.4) is very dependent on initial conditions as can be seen in Figure 1. Also (3.5) corroborates the well known fact [28] that bubbles propagate asymptotically in time at the speed of light in the thin wall limit of $\Lambda \ll 3\sigma$.

A space with positive curvature only makes sense if $a(0) \geq \frac{1}{RH}$. Once the initial value exceeds this critical value the space expands forever. The effect of the curvature becomes

eventually negligible. Thus it is not surprising that the evolution of the bubble is similar regardless of the curvature. There is a difference in the possible asymptotic value that x can take; in the positive curvature case x always has to remain below R . The rate of the expansion is asymptotically given by B in the shell coordinates and by H in the outside coordinates. In terms of the inside coordinates the motion of the bubble is given by:

$$Z(T) = \frac{1}{B} \sqrt{1 + B^2(T - T_0)^2}$$

This expression can be derived from the metric matching condition at the shell (7.3) and assuming that $b(T_0) = 1$, which is a good assumption when $\Lambda_{in} = 0$. T_0 is the inside time at which the bubble is created. For late times the bubble propagates at the speed of light as expected [28]. Ultimately, we are always interested in the motion of the bubble as viewed by the observer inside the bubble. The moral of this example is that the motion, as viewed by the inside observer, is the same regardless of the amount of curvature outside the bubble.

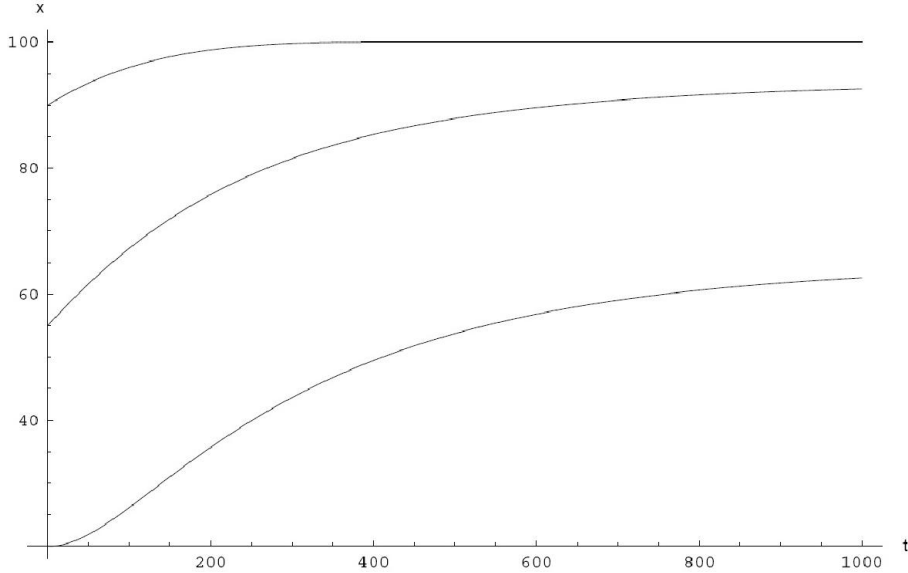


Figure 1: Time evolution of the bubble in the outside coordinates, $x[t]$, for several initial sizes, $x_{init} = 20, 55, 90$. The background is assumed homogeneous ($R = 100$) and without matter.

In our equations above (and in the ones that follow) we have chosen the natural units $c = 8\pi G = 1$. Since we are dealing only with classical evolutions, \hbar never comes up, so we have the freedom to pick one more unit. In the numerical evolution that we will undertake later, this means that there is rescaling of the coordinates (by a dimensionful parameter) that we are still free to do. We need to make sure that the scales involved do not cross the Planck scale because that would invalidate our classical analysis. We will always choose our various independent parameters (like Λ , σ , A) to be within a few orders of magnitude of each other, to ensure that their relative scales are not Planckian. The actual values themselves

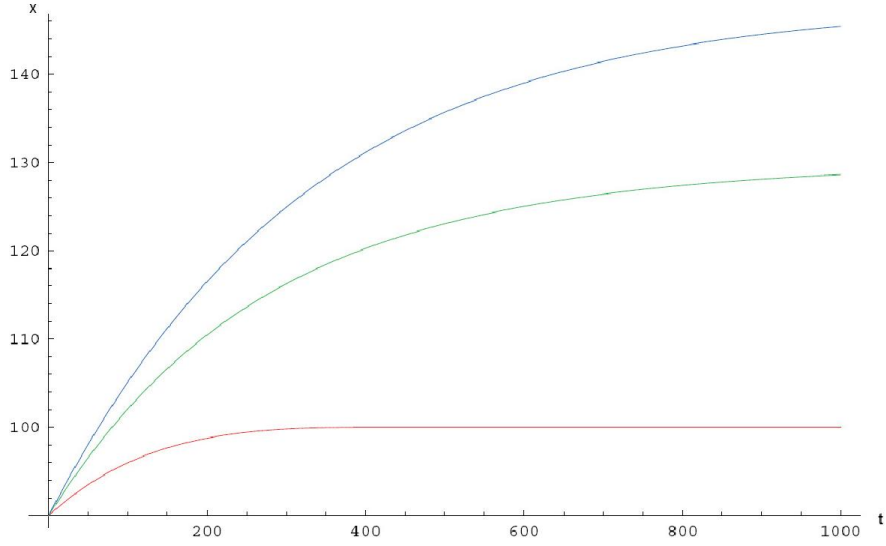


Figure 2: Time evolution of the bubble in the outside coordinates, $x[t]$, in homogeneous backgrounds without matter. Colors correspond to different choices of R ; $R = 100$ red, $R = 150$ green, $R = \infty$ blue.

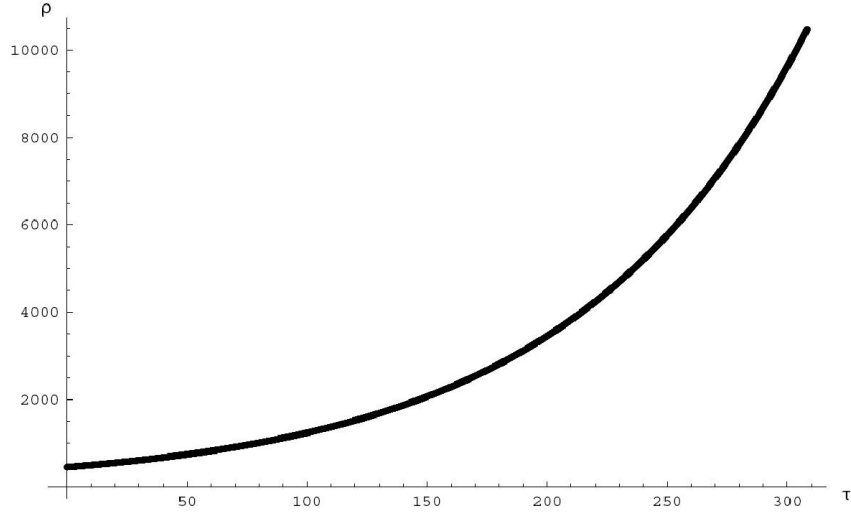


Figure 3: Time evolution of the bubble in the coordinates of the bubble, $\rho[\tau]$, in homogeneous backgrounds without matter (same as in Figure 2).

are not too relevant because of the above-mentioned freedom in choosing the scale for the coordinates.

Physically we expect the cosmological constant to reflect the scale corresponding to the minimum of some effective scalar potential, whereas the bubble stress-tensor should reflect the potential barrier between the two minima. So in principle it is not inconceivable that

for a sufficiently near-zero cosmological constant, the barrier height be many, many orders of magnitude bigger than the cosmological constant. But for a generic potential, we expect that the scales involved will be roughly of the same order, so we do not consider this scenario here.

As far as the evolution of the shell goes, the only place where we could have trans-Planckian effects becoming significant is when there is a singularity in the spacetime itself. In particular the fact that the shell surface is an actual physical wall, and *not* a surface at conformal infinity (like a horizon), means that we do not have to worry about finite energy modes observed far away being red-shifted trans-Planckian modes [29, 30, 31, 32].

The effects of curvature on the bubble propagation, as seen by the outside observer, are illustrated in Figures 1, 2 and 3. To simulate these evolutions we have chosen the following values for the parameters, in units of $8\pi G = 1$:

$$\begin{aligned}\Lambda &= 3 \times 10^{-5} \\ a_{init} &= 5 \\ \gamma_{out} &= \gamma_{in} = +1 \\ \sigma_{init} &= 10^{-3}\end{aligned}\tag{3.6}$$

These values for the parameters can not be chosen independently since they have to satisfy the condition (7.28) that yields:

$$\sigma \leq 2\sqrt{\frac{\Lambda}{3}} = 6.3 \times 10^{-3}\tag{3.7}$$

Also from the equation (3.1) the lower and the upper bound on x are:

$$\frac{1}{aB} \leq x \leq R\tag{3.8}$$

We have chosen the initial size of the bubble in accordance with this range.

In particular, Figure 1 shows the evolution of the bubble in the outside coordinates for various initial sizes. Note that the maximum size of the bubble in these coordinates corresponds to the limit $x = R$.

Figure 2 shows the effects of curvature on bubble propagation by comparing evolutions of bubbles with the same initial size x_{init} , but in different curvature background. We see that more curvature corresponds to a slower evolution of the bubble in the outside coordinates; however, the corresponding bubble evolution $\rho[\tau]$ in the bubble coordinates is exactly the same, irrespective of the amount of background curvature, and it is shown in Figure 3.

In addition, one might wonder what would happen if we did not assume the bubble to be a vacuum bubble, namely if $w \neq -1$. Then the evolution of the energy density σ on the bubble is governed by (7.24). In the absence of dust on the outside the solution to this equation is:

$$\sigma = \frac{\zeta}{\rho^{2(1+w)}}\tag{3.9}$$

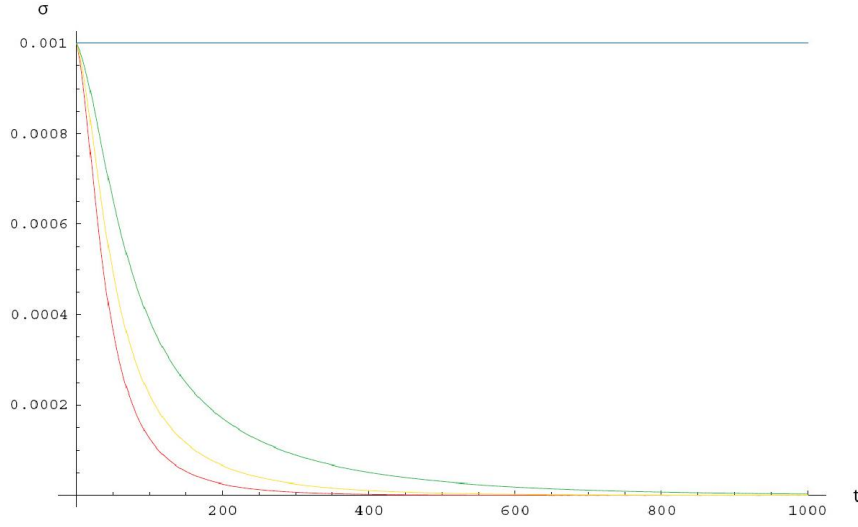


Figure 4: Time evolution of the surface energy density $\sigma[t]$ on the bubble. The background is assumed homogeneous ($R = 100$) and without matter. Colors correspond to different equations of state; $w = 1/3$ red, $w = 0$ yellow, $w = -1/3$ green, $w = -1$ blue.

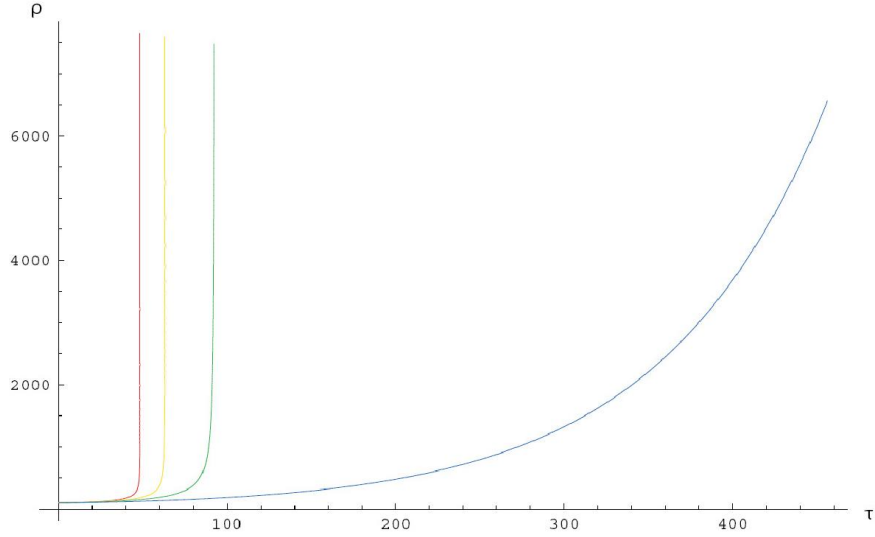


Figure 5: Time evolution of the bubble in the coordinates of the bubble, $\rho[\tau]$. The background is assumed homogeneous ($R = 100$) and without matter. Colors correspond to different equations of state; $w = 1/3$ red, $w = 0$ yellow, $w = -1/3$ green, $w = -1$ blue.

where ξ is a constant. When substituting this solution on (2.8) we obtain the following equation for $\rho(\tau)$

$$\dot{\rho}^2 = -1 + \left(\frac{\zeta}{4\rho^{(1+2w)}} + \frac{\Lambda}{3\zeta} \rho^{3+2w} \right)^2 \quad (3.10)$$

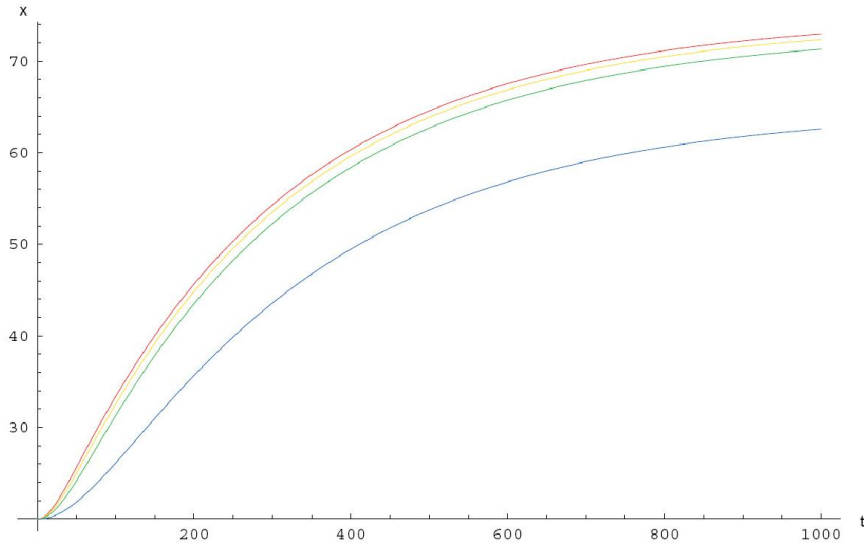


Figure 6: Time evolution of the bubble in the outside coordinates, $x[t]$. The background is assumed homogeneous ($R = 100$) and without matter. $x_{init} = 20$. Colors correspond to different equations of state; $w = 1/3$ red, $w = 0$ yellow, $w = -1/3$ green, $w = -1$ blue.

For ρ large, the solution to this equation takes the form:

$$\rho(\tau) \sim \frac{\rho(\tau_0)}{\left[1 - (1 + 2w)\frac{\Lambda}{3\zeta}\rho(\tau_0)^{1+2w}(\tau - \tau_0)\right]^{1/(1+2w)}} \quad (3.11)$$

This analysis of the asymptotic behavior is also captured in the results plotted in Figure 4, and Figure 5.

Figure 6 depicts the corresponding bubble evolution in the outside coordinates, $x[t]$.

In summary, in this section we have considered a closed FRW background that will eventually asymptote to a de Sitter space. The outside curvature doesn't affect the evolution of the vacuum bubbles when this is described in the shell coordinates, and hence neither does the evolution from the point of view of the inside coordinates. The curvature only makes a difference when the evolution is studied in terms of the outside coordinates. In these coordinates, the effect of a bigger curvature is to slow down the evolution of the comoving bubble coordinate. The asymptotic value of this coordinate depends on the initial condition but is always smaller than the curvature radius. When the equation of state of the shell is not that of vacuum, the evolution in the shell coordinates is much faster than that of vacuum but is also independent of the outside curvature. When described from the point of view of the outside coordinates this evolution although faster than the corresponding one for vacuum is qualitatively similar.

3.2 Homogeneous Background with Matter

To study the evolution of the bubble in a space that might contract we have to modify the

outside energy density. One option is to introduce matter. In this instance the evolution of the scale parameter is given by

$$\left(\frac{da}{dt}\right)^2 + \frac{1}{R^2} - \frac{\Lambda}{3}a^2 - \frac{A}{a} = 0$$

If $A \leq \frac{1}{R^3} \sqrt{\frac{4}{9\Lambda}}$ and $a(0)$ is small enough the expansion of the universe will reverse into contraction. With this new form of outside energy density, however, it is no longer consistent with the matching conditions to have a constant surface energy density on the bubble, not even when $\sigma + P = 0$. The evolution will be given by the equations:

$$\frac{dx}{dt} = \frac{-\left(1 - \frac{x^2}{R^2}\right) \frac{da/dt}{a} \pm \sqrt{\left(1 - \frac{x^2}{R^2}\right) (a^2 B^2 x^2 - 1) \left(B^2 - \left(\frac{\Lambda}{3} + \frac{A}{a^3}\right)\right)}}{xa^2 \left(B^2 - \frac{1}{a^2 R^2}\right)} \quad (3.12)$$

$$\frac{d\sigma}{dt} = -2 \left(\frac{da/dt}{a} + \frac{dx/dt}{x} \right) (\sigma + P) + \gamma_{out} \frac{dx/dt}{\sqrt{-(dx/dt)^2 a^2 + 1 - \frac{x^2}{R^2}}} \frac{3A}{a^2} \quad (3.13)$$

$$B = \frac{\sigma}{4} + \frac{1}{\sigma} \left(\frac{\Lambda}{3} + \frac{A}{a^3} \right) \quad (3.14)$$

As in the previous section in order to solve these equations an assumption about the equation of state on the bubble was needed. We did make the assumption that the shell is made of a perfect fluid with equation of state $P = w\sigma$, and explored several values for w . For the dust energy to be comparable to the cosmological constant at early times, we choose

$$A = 10^{-4} \quad (3.15)$$

in Planck units. The critical curvature which is the minimal curvature needed for the space to turn around and eventually collapse is given by:

$$R_{cr} = \left(\frac{9\Lambda A^2}{4} \right)^{-1/6} = 107 \quad (3.16)$$

The position of the maximum of the potential $V[a]$ is given by:

$$a_{max} = \left(\frac{3A}{2\Lambda} \right)^{1/3} = 1.7 \quad (3.17)$$

In our simulations we choose the initial value of the scale factor a to be $a_{init} = a(0) = 1$.

The outside background geometry will be completely specified once we choose the amount of curvature. We will consider several cases.

3.2.1 $R > R_{cr}$

The universe will always expand. If at the instant the bubble is created $a(0)$ is to the left of max of the potential (2.4), then the universe will experience a period of slower growth until it eventually goes over the max and the expansion becomes dominated by the cosmological constant.

We will now investigate bubble propagation on such background. We are again assuming that the inside region has zero energy density, and that $\gamma_{out} = \gamma_{in} = +1$. In this case, the condition (7.28) yields:

$$\sigma \leq 2\sqrt{\frac{\Lambda}{3} + \frac{A}{a^3}} \quad (3.18)$$

This constraint will be the strongest as $a \rightarrow \infty$, when, as is the case without matter, it reduces to:

$$\sigma \leq 6.3 \times 10^{-3} \quad (3.19)$$

Once again, we choose:

$$\sigma_{init} = 10^{-3} \quad (3.20)$$

where σ_{init} is given in Planck units. From the equation (3.12) the lower and the upper bound on x are:

$$\frac{1}{aB} \leq x \leq R \quad (3.21)$$

We will choose the initial size of the bubble in accordance with this range and compare the evolution for several equations of state on the surface of the bubble. Decreasing R (and therefore increasing the curvature of the space) will have the effect of slowing down the evolution, as long as $R > R_{cr}$.

First let us consider the case with very little curvature, $R = 500$. Figure 7 shows the time evolution of bubbles of several initial sizes in the outside coordinates. In most cases bubbles grow without reaching the upper bound, $x = R$. Smaller w slows down the expansion rate, and in particular, the choice of $w = -1$ soon leads to a contracting bubble in the outside coordinates. Depending on the initial size of the bubble, $w = -1$ bubbles either reach the lower bound, $x = \frac{1}{aB}$, which results in the breakdown of the simulation, or eventually stabilize and stop contracting.

Time evolution in the coordinates on the bubble (Figure 8) reveals behavior similar to the case without matter. Namely, for the bubbles that do survive, the evolution is slower than in the case without matter, but the overall qualitative behavior stays the same.

Next we turn to the case with more curvature, but still such that $R > R_{cr}$. From Figure 9 we see that in most cases bubbles again grow, but now they asymptote to the upper bound, $x = R$.

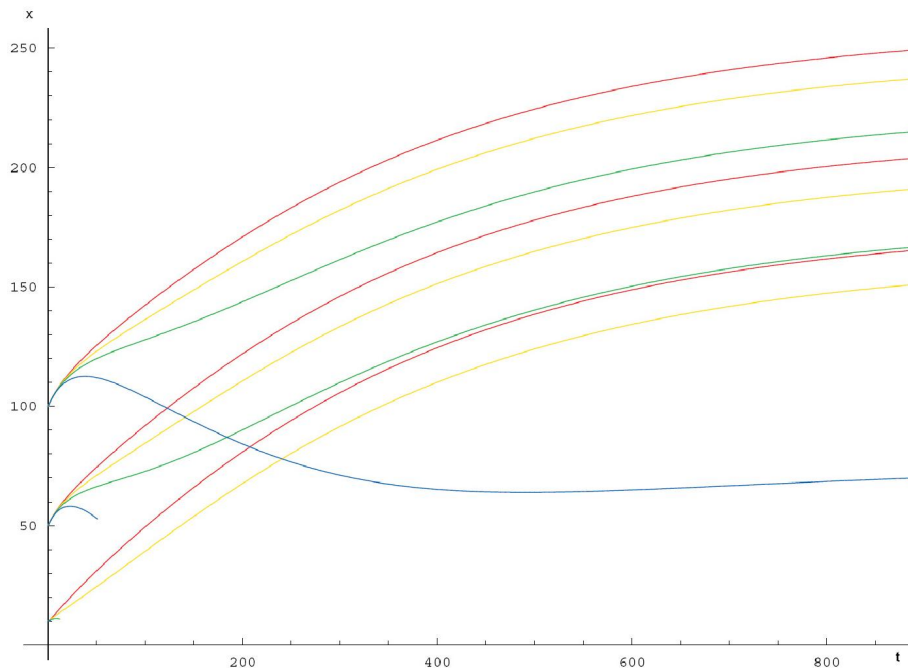


Figure 7: Time evolution of the bubble in the outside coordinates, $x[t]$, for several initial sizes, $x_{init} = 10, 50, 100$. The background contains homogeneous curvature ($R = 500$) and matter ($A = 10^{-4}$). Colors correspond to different equations of state; $w = 1/3$ red, $w = 0$ yellow, $w = -1/3$ green, $w = -1$ blue.

The corresponding bubble evolution in the coordinates on the bubble is shown in Figure 10. The overall effect of more curvature is a further slowdown in the time evolution of the bubbles.

In summary, in this section we have considered a closed FRW background that contains dust as well as a cosmological constant but that will eventually asymptote to a de Sitter space. In this case it is no longer consistent to have vacuum shells separating the interior and exterior region³. We have studied the motion for different values of w . In shell coordinates, for $w = -1$, we have found that some bubbles do eventually become subcritical or stabilize and stop contracting.

3.2.2 $R < R_{cr}$

For curvature greater than the critical value (i.e. $R < R_{cr}$) the space will eventually collapse. To investigate this case we choose $R = 100$. The evolution of the scale factor is shown in Figure 11.

³The point of this section is to consider bubble creation for times sufficiently small for the dust density to make a difference. For long times the dust density will redshift and this background will become indistinguishable from the previous one.

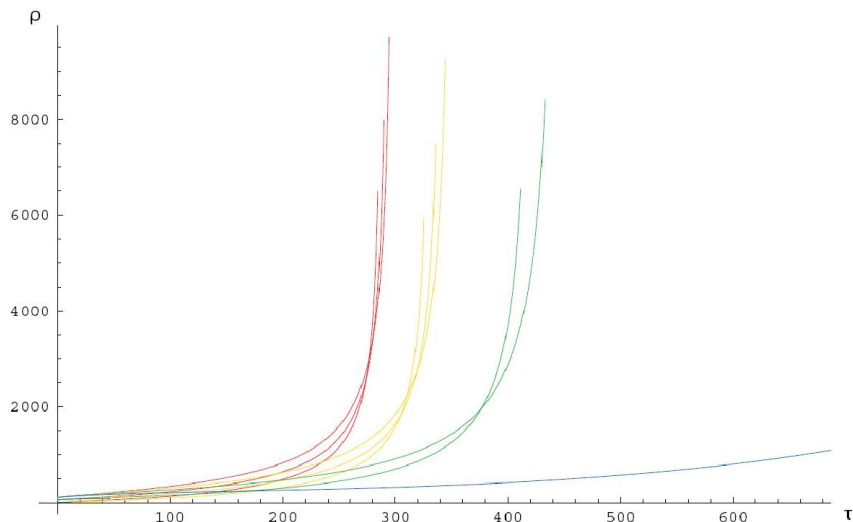


Figure 8: Time evolution of the bubble in the bubble coordinates, $\rho[t]$, for the same background conditions as in Figure 7. Colors correspond to different equations of state; $w = 1/3$ red, $w = 0$ yellow, $w = -1/3$ green, $w = -1$ blue.

In the outside coordinates, the time evolution of most bubbles will once again lead to the upper bound, $x = R$ (Figure 12). Bubbles with $w = -1$ contract and hit the lower bound $x = \frac{1}{aB}$, which stops their further evolution.

Figure 13 reveals corresponding behavior in the coordinates on the bubble. Bubbles which do not hit the bound $x = \frac{1}{aB}$ eventually collapse along with the collapse of the space itself.

In summary, in this section we have considered a closed FRW background that contains dust and a cosmological constant and that will eventually contract. As in the previous case it is not longer consistent to have vacuum shells separating the inside and outside region. Depending on the initial size, bubbles with smaller value of w become subcritical and disappear while the others continue to grow and eventually collapse along with the space itself.

4. Bubble Expansion in Inhomogeneous Background

4.1 Generating a Curvature Profile

In order to generate an inhomogeneous curvature profile, we choose:

$$R(r) = (\alpha r + \beta R_{cr}) \left(1 \pm \frac{1}{\gamma + (\delta - r)^2} \right) \quad (4.1)$$

$\alpha > 0$ ensures that as $r \rightarrow \infty$ we have an asymptotically flat space. Choosing $\beta > 1$ will allow us to generate a sharp drop in the function $R(r)$, for the cases where the minus sign

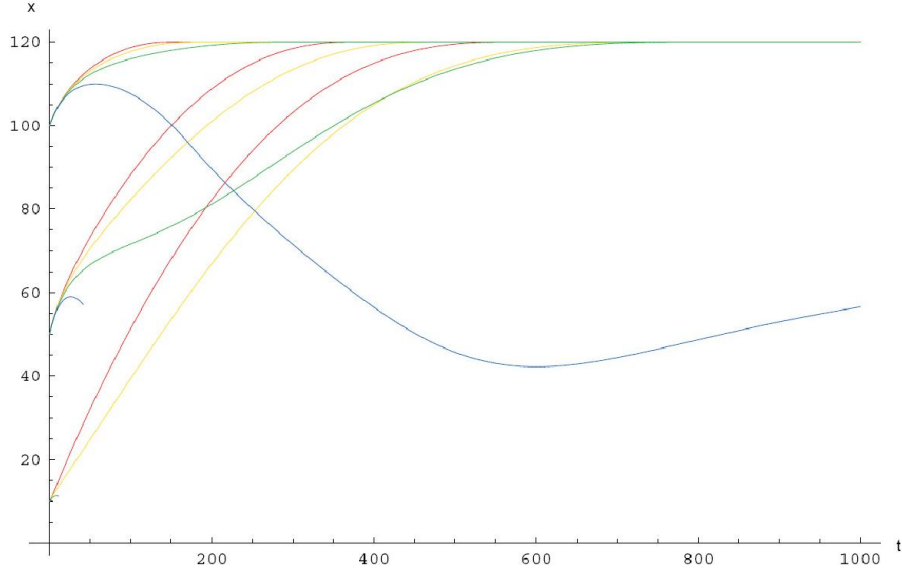


Figure 9: Time evolution of the bubble in the outside coordinates, $x[t]$, for several initial sizes, $x_{init} = 10, 50, 100$. The background contains homogeneous curvature ($R = 120$) and matter ($A = 10^{-4}$). Colors correspond to different equations of state; $w = 1/3$ red, $w = 0$ yellow, $w = -1/3$ green, $w = -1$ blue.

is chosen. The position and the width of the extremum will be regulated by the parameter δ , and the depth/height by γ . Since we do not want our space to crunch anywhere, we will require $R(r) > R_{cr}$ for all r .

Furthermore, we want to make sure to satisfy the weak energy condition, namely that the matter density stays positive:

$$d(t, r) = \frac{3A}{a^2(t, r)(a(t, r) + ra'(t, r))} \quad (4.2)$$

Since A is positive definite, this gives us a condition:

$$a(t, r) + ra'(t, r) > 0$$

This means that $a(r)$ should nowhere fall faster than $1/r$.

4.2 Examples

As an example, we first choose the minus sign in $R(r)$, with $\alpha = 0.1$, $\beta = 3$ and $\delta = 20$. In order for R to stay above R_{cr} , in this case we need $\gamma > 1.5$. In addition, numerical simulations show that to satisfy the weak energy condition, $\gamma \geq 2.9$, and since we'd like to investigate the sharpest possible profile, we choose $\gamma = 2.9$.

This choice of the function $R(r)$ generates a profile in the evolution of the scale factor $a(r, t)$, as shown in Figure 14. We will compare evolution of a bubble in such background with evolution in a curvature background without a profile, namely, $R(r) = (0.1r + 3R_{cr})$.

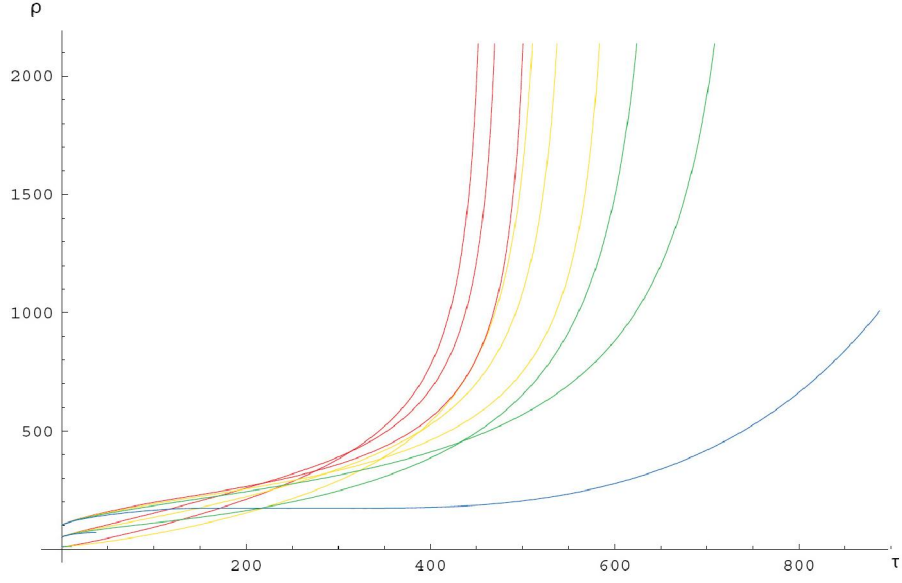


Figure 10: Time evolution of the bubble in the bubble coordinates, $\rho[t]$, for the same background conditions as in Figure 9. Colors correspond to different equations of state; $w = 1/3$ red, $w = 0$ yellow, $w = -1/3$ green, $w = -1$ blue.

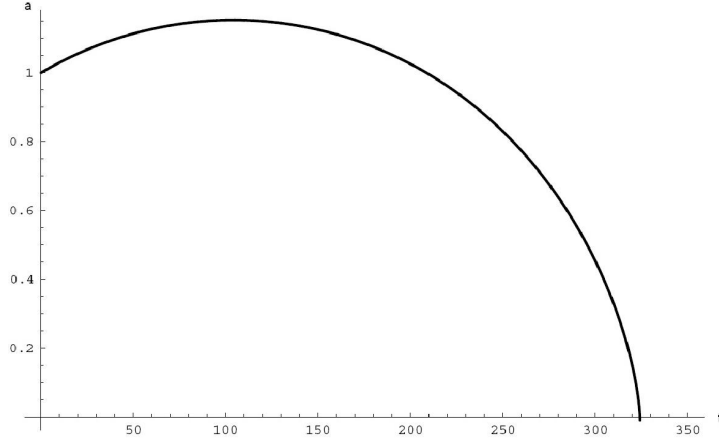


Figure 11: Time evolution of the scale factor $a[t]$ for $R = 100$. ($\Lambda = 3 \times 10^{-5}$, $A = 10^{-4}$.)

The two choices of $R(r)$ are shown in Figure 15. The resulting bubble evolutions are shown in Figures 16 and 17. We see that even though in the outside coordinates bubble evolution is greatly affected by the curvature profile, such effect is absent for the bubble evolution in the coordinates on the bubble.

For comparison, we will also choose $R(r)$ with the plus sign, and $\alpha = 0.1$, $\beta = 2$, $\gamma = 0.7$ and $\delta = 20$, depicted in Figure 19. This results in a profile for $a(r, t)$ shown in Figure 18.

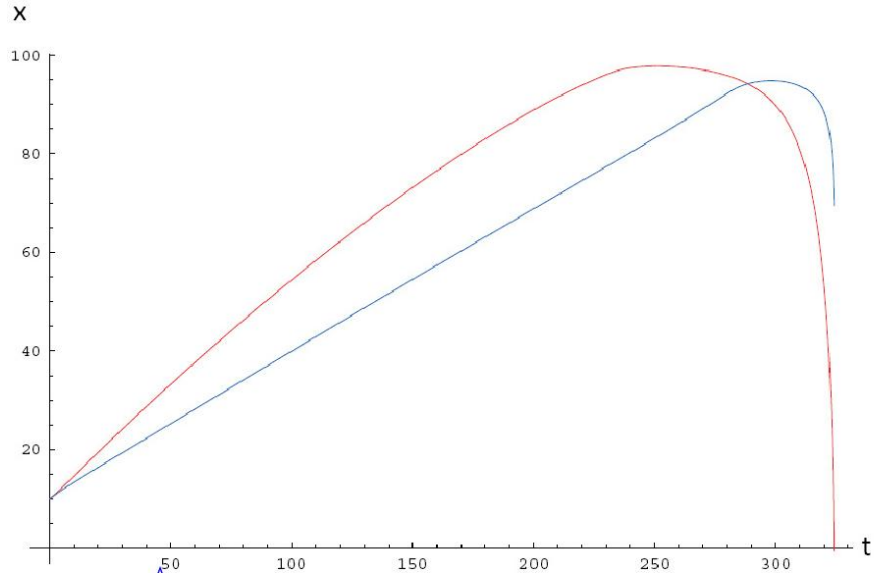


Figure 12: Time evolution of the bubble in the outside coordinates, $x[t]$, for crunching background (Figure 11). $x_{init} = 10$. $R = 100$. Colors correspond to different equations of state: $w = 1/3$ red, $w = 0$ blue.

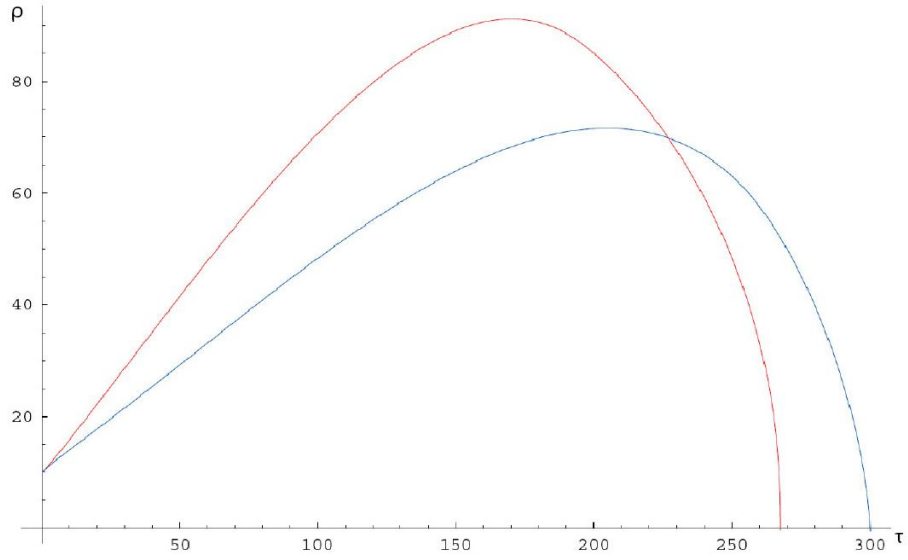


Figure 13: Time evolution of the bubble in the bubble coordinates, $\rho[t]$, for crunching background (Figure 11). $x_{init} = 10$. $R = 100$. Colors correspond to different equations of state; $w = 1/3$ red, $w = 0$ blue.

The corresponding bubble evolution is shown in Figures 20 and 21.

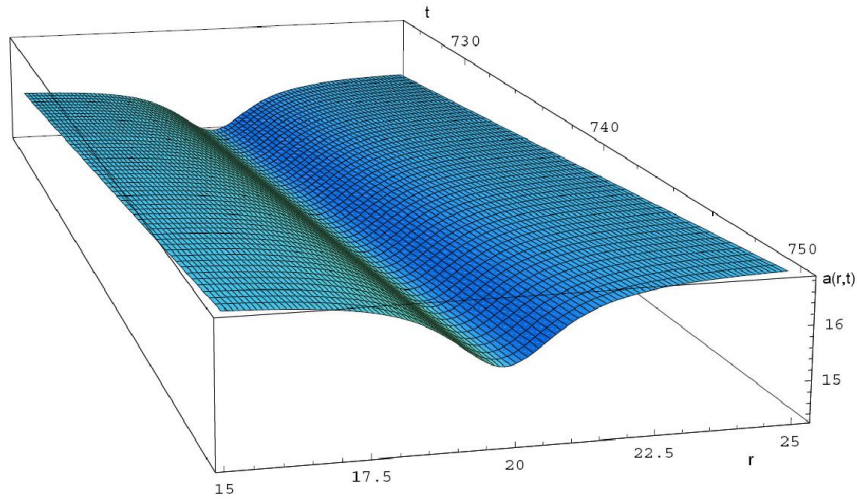


Figure 14: $a(r, t)$ for curvature background depicted in red in Figure 15.

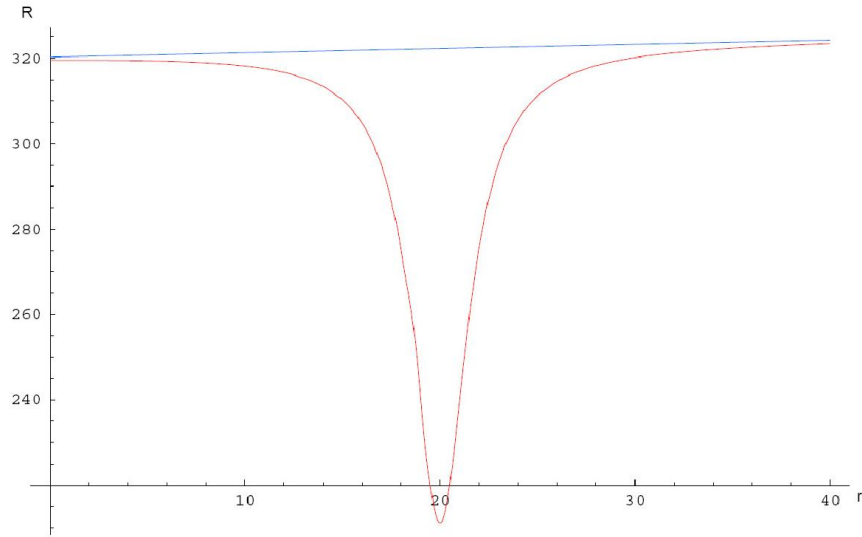


Figure 15: First example of an inhomogeneous background: Two choices of $R(r)$.

5. Conclusions

We have examined the evolution of bubbles of true vacuum in several backgrounds (that always include a cosmological constant) to assess the effect of curvature on the propagation. The effect of curvature does seem to qualitatively change the bubble evolution when looked at in terms of the outside coordinates, but it does not seem important when the evolution is studied in terms of the more physically relevant coordinates on the shell or its interior. In the presence of matter, we observe that some bubbles, with an equation of state close to $w = -1$,

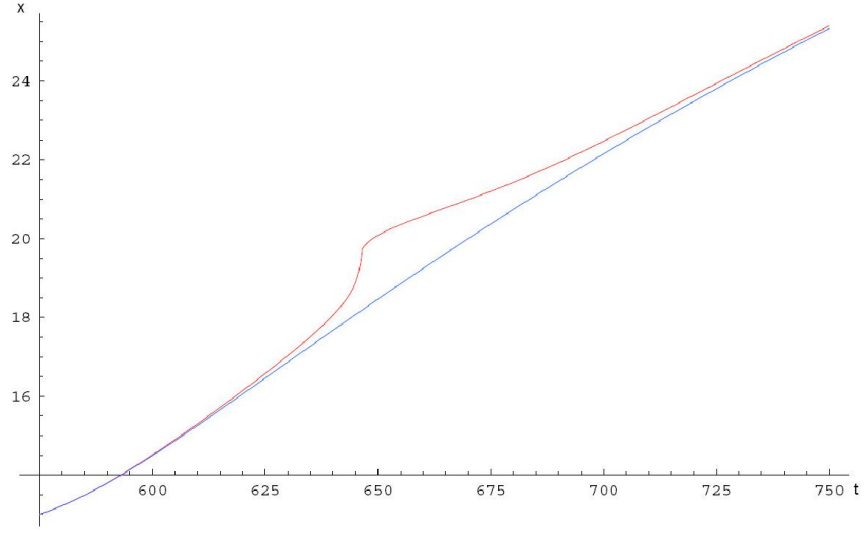


Figure 16: Evolution of bubbles in outside coordinates, $x(t)$, for two curvature profiles shown in Figure 15.

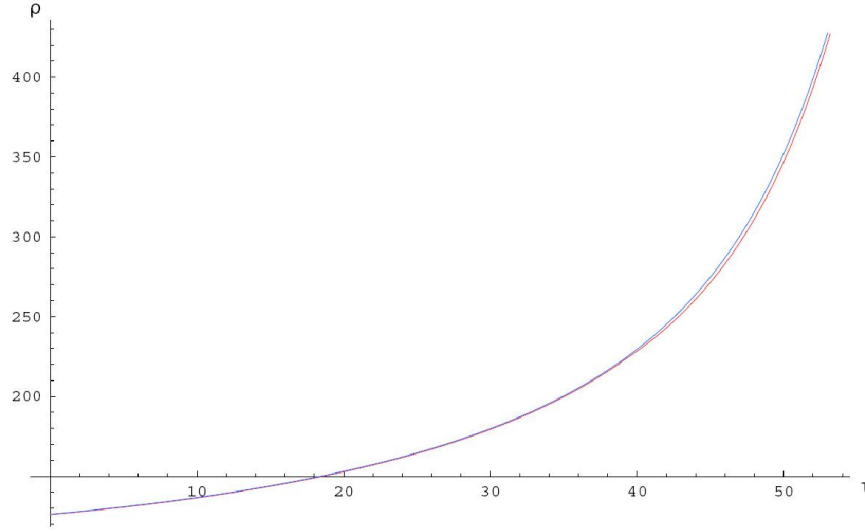


Figure 17: Evolution of bubbles in bubble coordinates, $\rho(\tau)$, for two curvature profiles shown in Figure 15.

disappear. Those that survive do behave qualitatively the same.

The explanation for this insensitivity to inhomogeneities is to be found in the weak energy condition: our background spacetime is consistent only when (4.2) is positive, which restricts the sharpness of the inhomogeneity profiles that are allowed. This could of course

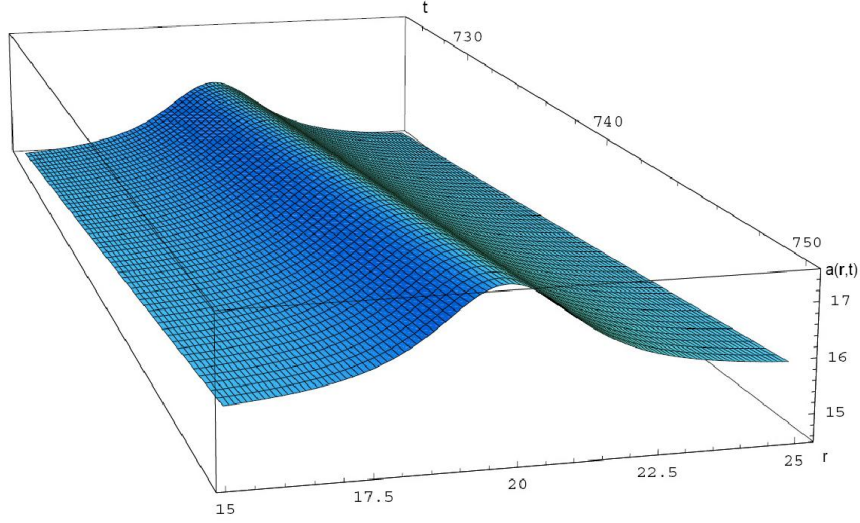


Figure 18: $a(r, t)$ for curvature background depicted in red in Figure 19.

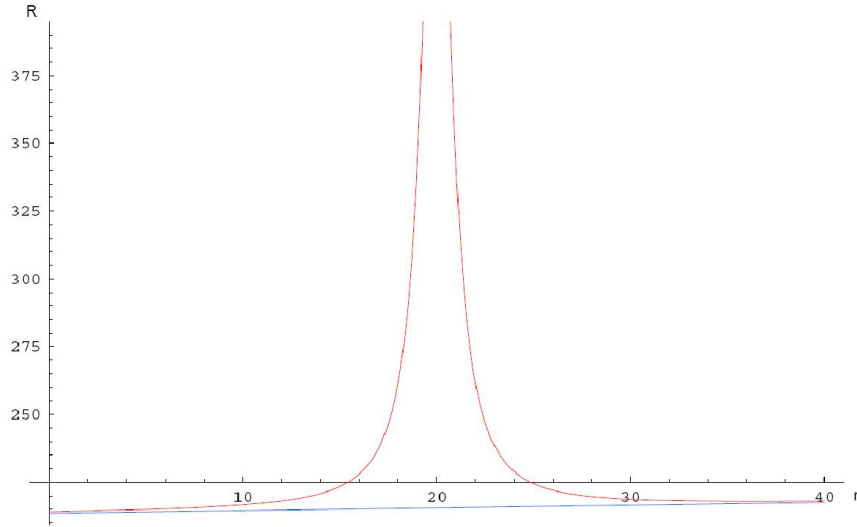


Figure 19: Second example of an inhomogeneous background: Two choices of $R(r)$.

be a restriction arising from the ansatz for the background that we are working with. But it should be mentioned that in the work of Wald [11] that was mentioned in the introduction, the energy conditions played a crucial role in the proof of the cosmic no hair theorem for anisotropic (but homogeneous) cosmologies.

We view this work as an attempt to test the requirements to arrive at a universe like ours without making the simplifying assumptions of starting with an FRW metric. There

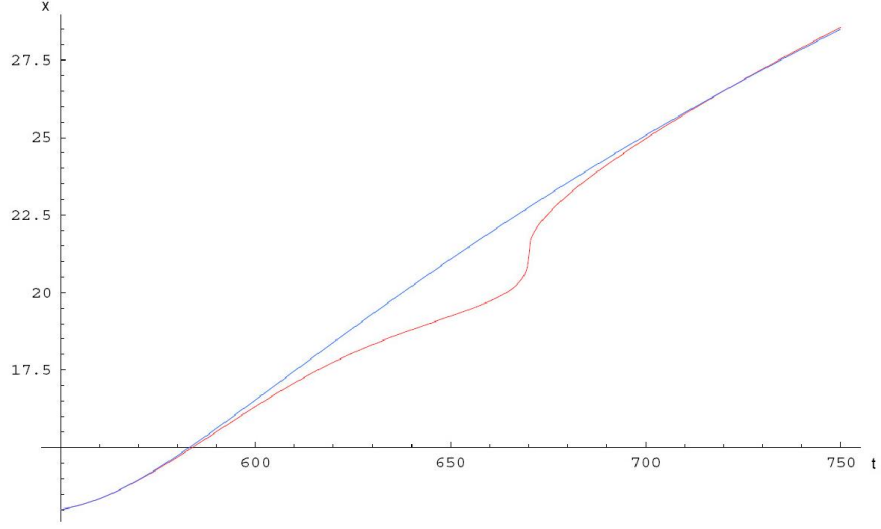


Figure 20: Evolution of bubbles in outside coordinates, $x(t)$, for two curvature profiles shown in Figure 19.

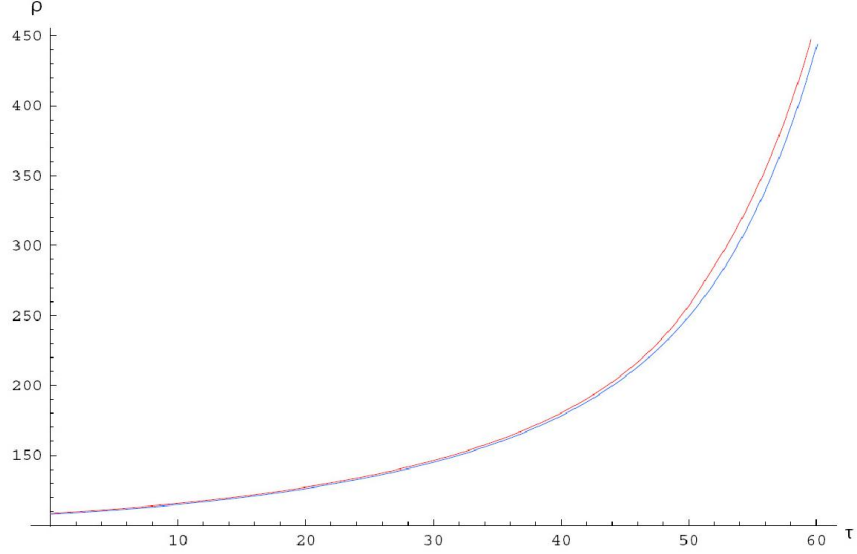


Figure 21: Evolution of bubbles in bubble coordinates, $\rho(\tau)$, for two curvature profiles shown in Figure 19.

are many directions in which the work here can be extended. We have examined only a few inhomogeneity profiles here, a more thorough understanding of the evolution curves in more generic situations is certainly of interest. If we think of our setup as a toy model for inflation, it will definitely be of interest to study the *genericity* of inflation in the space of possible

inhomogeneity profiles. Another important direction to follow is to evaluate the tunneling amplitudes for inhomogeneous ambient spaces. This is a notoriously difficult problem on which any enlightenment will be welcome.

Another problem that is of interest in this context is whether there are signatures left on the new (inside) Universe due to the propagation of the bubble through the inhomogeneous ambience. The bubble can be thought of as a Casimir cavity with a moving wall and the cavity radiation (the analogue of the CMB in this context) will carry imprints of the external inhomogeneities. Because of the spherical symmetry, this is effectively a two-dimensional QFT problem, with moving mirror boundary conditions [37].

6. Acknowledgments

CK would like to thank Frank Ferrari for useful discussions, and the audience at the Joint ULB-VUB-KUL-Solvay seminar for feedback on a talk based on this paper. The work of CK is supported in part by IISN - Belgium (convention 4.4505.86), by the Belgian National Lottery, by the European Commission FP6 RTN programme MRTN-CT-2004-005104 in which CK is associated with V. U. Brussel, and by the Belgian Federal Science Policy Office through the Interuniversity Attraction Pole P5/27.

The work of W. Fischler, S. Paban and M. Žanić is partially supported by the National Science Foundation under Grant No. PHY-0455649.

7. Appendix

In this appendix, we will derive the coupled differential equations that form the starting point for our numerical shell evolution plots. These equations are a direct consequence of Israel's junctions conditions⁴, which relate the discontinuity in the extrinsic curvature *across* the shell surface to the energy-momentum layer *on* the shell. The general expressions for these equations for the case of spherically symmetric junctions can be found in, e.g., [2]. Here we discuss a few of the ingredients that go into our specific problem by doing some illustrative computations *ab initio*. The aim is to stress some issues like choices of signs and coordinates which are often not adequately addressed in the literature.

We will work with the mostly minus $\{+, -, -, -\}$ metric, and the signs on the energy-momentum tensor for the ideal fluid are fixed by

$$T_{\alpha}^{\beta} = (\epsilon + p)u_{\alpha}u^{\beta} - p\delta_{\alpha}^{\beta}. \quad (7.1)$$

Einstein's equation takes the form $G_{\alpha\beta} = T_{\alpha\beta}$, in natural units ($8\pi G = c = 1$). Later, when we work with quantities defined on the shell, we will have analogous sign conventions for them as well. Throughout, Latin indices denote 3-dimensional objects defined on the shell

⁴A pedagogical derivation of the junction conditions based on a distributional approach to Einstein's equations can be found in [33].

hypersurface, Greek indices stand for 4-dimensional quantities, and semi-colon is shorthand for the covariant derivative. We will also need $e_a^\alpha \equiv \frac{\partial x^\alpha}{\partial y^a}$, which are projectors (pull-backs) that can be used to project a 4-quantity on to the 3-surface.

The first of Israel's two conditions says that the metric induced on the shell from the bulk 4-metrics on either side should match, and be equal to the 3-metric on the shell. The assumption of spherical symmetry restricts the form of the intrinsic metric on the shell to the form,

$$ds_3^2 = d\tau^2 - \rho(\tau)^2 d\Omega_2, \quad (7.2)$$

where τ is the only independent coordinate on the shell, which we take to be the shell proper time. So looked at from the outside, on the shell, we can parametrize the coordinates as $r = x(\tau)$ and $t = t(\tau)$, and from the inside, $T = T(\tau)$ and $z = z(\tau)$. Since the metric from either side on the shell should agree with the 3-metric on the shell, we get two conditions from the inside (open-FRW),

$$b(T)z = \rho(\tau), \quad \left(\frac{dT}{d\tau}\right)^2 = 1 + \frac{b(T)^2}{1+z^2} \left(\frac{dz}{d\tau}\right)^2, \quad (7.3)$$

and two from the outside (LTB),

$$a(t, x)x = \rho(\tau), \quad \left(\frac{dt}{d\tau}\right)^2 = 1 + \frac{(a(t, x)x)_{,x}^2}{1 - x^2/R(x)^2} \left(\frac{dx}{d\tau}\right)^2. \quad (7.4)$$

All the variables in these equations are thought of as functions of τ .

Now we turn to the second junction conditions, which determine the dynamics of the shell. These are expressed in terms of the extrinsic curvature:

$$K_{ab} = n_{\alpha;\beta} e_a^\alpha e_b^\beta. \quad (7.5)$$

Here n_α is the outward normal to the surface under question (since we are working with a closed shell, there is no ambiguity in making this choice). There are many different choices and sign conventions for the extrinsic curvature in the literature, we have made the above definitions so that the extrinsic curvature of a 2-sphere is positive. In particular, this differs from [2], but is in agreement with most of the other references/reviews on the subject [33, 34, 35, 36]. With these prescriptions, the second junction condition takes the form

$$[K_{ab}] - h_{ab}[K] = S_{ab}, \quad (7.6)$$

with h_{ab} denoting the shell metric, which in our case is (7.2). The 3-tensor S_{ab} stands for the surface energy-momentum tensor, and we will assume it to have a perfect-fluid form analogous to (7.1). Square brackets stand for discontinuities across the shell: $[K] = K_{out} - K_{in}$.

It can be shown [2], that the junctions conditions imply a conservation law of the form

$$S_a^b{}_{;b} + [e_a^\alpha T_\alpha^\beta n_\beta] = 0, \quad (7.7)$$

where $T_{\alpha(out/in)}^\beta$ is the bulk energy-momentum tensor on either side. The advantage of this equation is that it is first order, and one can exchange⁵ one of the second order equations arising from the junction conditions with (7.7). This is indeed what we will do.

Because of spherical symmetry and the form of the three metric, the extrinsic curvature K_a^b has independent components K_τ^τ and $K_\theta^\theta = K_\phi^\phi$, while the surface energy tensor S_a^b contains $S_\tau^\tau \equiv \sigma$ and $S_\theta^\theta = S_\phi^\phi \equiv -P$. So the independent relations that arise from the second junction conditions are

$$-\frac{\sigma}{2} = [K_\theta^\theta], \quad (7.8)$$

$$P = [K_\tau^\tau] + [K_\theta^\theta]. \quad (7.9)$$

Both σ and P are purely functions of τ by spherical symmetry. The conservation law (7.7) takes the form,

$$\frac{d\sigma}{d\tau} + \frac{2}{\rho} \frac{d\rho}{d\tau} (\sigma + P) + [T_\tau^n] = 0, \quad (7.10)$$

where $[T_\tau^n] \equiv [e_\tau^\alpha T_\alpha^\beta n_\beta]$. The evolution of the shell is completely determined by (7.8) and (7.10), so our task then is to write down these differential equations explicitly so that we can proceed with the numerics.

We have different sets of coordinates in each of the three regions, but not all of these coordinates can be explicitly written in terms of the others. So we will write the matching conditions in terms of the LTB coordinates. The LTB metric is known only numerically (see (2.2), (2.4)), so there is no hope of writing it in terms of the other coordinates, thereby making this choice inevitable. Since the evolution is best understood in the shell coordinates, once we have the evolution curves in LTB coordinates, we will translate them numerically to $\rho(\tau)$.

We start with (7.8). To calculate the extrinsic curvatures, we need the normal vectors in the corresponding coordinates. We will start with the LTB side where the coordinates are $x^\alpha = (t, x, \theta, \phi)$. The projectors are:

$$u^\alpha \equiv e_\tau^\alpha = \left(\frac{dt}{d\tau}, \frac{dx}{d\tau}, 0, 0 \right), \\ e_\theta^\alpha = (0, 0, 1, 0), \quad e_\phi^\alpha = (0, 0, 0, 1).$$

Since u^α is the 4-velocity of the bubble, the normal n_β will be determined (upto a sign) by the two conditions $u^\alpha n_\alpha = 0$ and $n^\alpha n_\alpha = -1$, where raising and lowering are done with the LTB metric. The second condition arises because our shell is timelike: a timelike shell is defined by a spacelike normal. A simple calculation yields,

$$n_\alpha = \gamma_{out} \left(\frac{-(ax)_{,x} \dot{x}}{\sqrt{(1-x^2/R^2)}}, \frac{(ax)_{,x} \dot{t}}{\sqrt{(1-x^2/R^2)}}, 0, 0 \right) \quad (7.11)$$

⁵This is analogous to the fact that the covariant energy conservation equation is an integrability condition for Einstein's equations.

where the dots are with respect to τ . The choice of sign for the normal is encoded in γ_{out} , and is fixed by the condition that the normal should point from the inside to the outside. For an expanding shell, this means that $\gamma_{out} = +1$. For a collapsing shell $\gamma_{out} = -1$.

Using these, the K_θ^θ on the LTB side turns out to be,

$$K_{\theta(out)}^\theta = h^{\theta\theta} n_{\theta;\theta} = \frac{1}{\rho^2} (n_{\theta;\theta} - \Gamma_{\theta\theta}^\alpha n_\alpha) = \gamma_{out} \left(\frac{(ax)_{,t} (ax)_{,x} \dot{x} + (1 - x^2/R^2) \dot{t}}{\rho \sqrt{(1 - x^2/R^2)}} \right). \quad (7.12)$$

We have used (7.4) to do some of the simplifications, and $(ax)_{,t}$ stands for $(x\partial_t a)$ because at this stage x and t are unrelated variables: when we eliminate τ to write x as a function of t , this will no longer be the case. Repeating the above calculation for K_θ^θ on the inside (open-FRW), with coordinates $x^\alpha = (T, z, \theta, \phi)$, we have

$$K_{\theta(in)}^\theta = \gamma_{in} \left(\frac{zb \frac{db}{dT} \dot{z} + (1 + z^2) \dot{T}}{\rho \sqrt{1 + z^2}} \right). \quad (7.13)$$

Again, $\gamma_{in} = +1$ when the radius of the inside region is increasing; otherwise, $\gamma_{in} = -1$. The junction condition becomes,

$$\gamma_{out} \left(\frac{(ax)_{,t} (ax)_{,x} \dot{x} + (1 - x^2/R^2) \dot{t}}{\rho \sqrt{(1 - x^2/R^2)}} \right) - \gamma_{in} \left(\frac{zb \frac{db}{dT} \dot{z} + (1 + z^2) \dot{T}}{\rho \sqrt{1 + z^2}} \right) = -\frac{\sigma}{2}. \quad (7.14)$$

By using (7.4), it is possible to rewrite this equation in a more standard form as:

$$\gamma_{out} \sqrt{\dot{\rho}^2 - \Delta_{out}} - \gamma_{in} \sqrt{\dot{\rho}^2 - \Delta_{in}} = -\frac{\sigma \rho}{2}, \quad (7.15)$$

where $\Delta_{out} = -(1 - x^2/R^2) + (ax)_{,t}^2$, and $\Delta_{in} = -(1 + z^2) + z^2 (db/dT)^2$. The quickest way to demonstrate this is to start with the final expressions. For instance, for the LTB piece, we can expand $\dot{\rho}$ as $(ax)_{,t} \dot{t} + (ax)_{,x} \dot{x}$, use the relation

$$1 - \frac{x^2}{R^2} = \frac{(ax)_{,x}^2 \dot{x}^2}{\dot{t}^2 - 1} \quad (7.16)$$

once, assemble a perfect square from the pieces, and then use (7.16) again to end up with the first piece in (7.14). Equation (7.16) here is just a rewriting of (7.4). An analogous transformation can be done for the open-FRW part of the equation.

The advantage of the form (7.15) is that now we can use the LTB equation of motion (resp. the open-FRW equation of motion) to simplify the two terms further to write

$$\Delta_{out} = -1 + \left(\frac{A}{a^3} + \frac{\Lambda_{out}}{3} \right) \rho^2, \quad (7.17)$$

$$\Delta_{in} = -1 + \frac{\Lambda_{in}}{3} \rho^2. \quad (7.18)$$

Now, we take up the task of writing these equations purely in the LTB coordinates, for otherwise, despite being correct, they will be of no practical value in computations because of the mixing of coordinates. Using (7.17) and (7.18), we can write (7.15) as

$$\dot{\rho}^2 = \rho^2 B^2 - 1, \quad (7.19)$$

where

$$B^2 = \frac{\Lambda_{in}}{3} + \left(\frac{\sigma}{4} + \frac{1}{\sigma} \left(\frac{\Lambda_{out} - \Lambda_{in}}{3} + \frac{A}{3} \right) \right)^2. \quad (7.20)$$

This form is useful because we just have to focus on $\dot{\rho}$ and ρ because everything else is already manifestly in LTB coordinates. The idea is that instead of choosing $\rho(\tau)$ as the curve for the bubble-evolution, we want to parametrize it as $x(t)$. Since x and t are dependent variables *on* the shell, this is legitimate. So we write $\rho = ax$, and rewrite $\dot{\rho}$ as

$$\dot{\rho} = \frac{\left(x \partial_t a + (ax)_{,x} \frac{dx}{dt} \right)}{\sqrt{1 - \frac{(ax)_{,x}^2}{1-x^2/R^2} \left(\frac{dx}{dt} \right)^2}}. \quad (7.21)$$

Using this in (7.19), and using the LTB equation of motion for $\partial_t a$, we end up with,

$$\frac{dx}{dt} = \frac{\left\{ -x \left(1 - \frac{x^2}{R^2} \right) \left(\frac{A}{a} + \frac{\Lambda a^2}{3} - \frac{1}{R^2} \right)^{1/2} \pm \right.}{(ax)_{,x} (a^2 x^2 B^2 - x^2/R^2)} \left. \pm x \left\{ \left(1 - \frac{x^2}{R^2} \right) (a^2 x^2 B^2 - 1) \left(a^2 B^2 - \frac{A}{a} - \frac{\Lambda a^2}{3} \right) \right\}^{1/2} \right\}} \quad (7.22)$$

This is the first of the two shell evolution equations (the other being (7.10)) in a form that is directly applicable for numerical simulations. The sign on the square root comes from the square root of (7.19) and has to be chosen according to whether the shell is expanding or contracting.

The second of the coupled shell-equations is easily translated into the LTB coordinates as well. On the LTB side, matter takes the form dust + cosmological constant (2.2). So, using (7.11),

$$T_{\tau(out)}^n \equiv e_\tau^t T_t^t n_t + e_\tau^x T_x^x n_x = - \frac{\gamma_{out}(ax)_{,x} \frac{dx}{dt} d(x,t) \sqrt{1 - x^2/R^2}}{1 - x^2/R^2 - (ax)_{,x}^2 (dx/dt)^2}. \quad (7.23)$$

On the inside, the only matter is the vacuum energy, which gives rise to $T_{\tau(in)}^n = 0$. These along with (7.4) can be used to write (7.10) in the form

$$\frac{d\sigma}{dt} + \frac{\left(x \partial_t a + (ax)_{,x} \frac{dx}{dt} \right)}{ax} (\sigma + P) - \frac{\gamma_{out}(ax)_{,x} \frac{dx}{dt} d(x,t)}{\sqrt{1 - \frac{x^2}{R^2} - (ax)_{,x}^2 (dx/dt)^2}} = 0. \quad (7.24)$$

Together with an equation of state relating σ to P , and the LTB equation of motion (2.2), (7.22, 7.24) comprise the starting point for the various special cases we study in the main text of this paper.

When solving for shell dynamics, we should demand that the positive energy condition be satisfied, that is

$$\sigma > 0. \quad (7.25)$$

Using the formulas derived here (in particular (7.15)), we can write :

$$\Delta_{out} - \Delta_{in} = \frac{\rho^2 \sigma^2}{4} + \gamma_{out} \rho \sigma (\dot{\rho}^2 - \Delta_{out})^{1/2}, \quad (7.26)$$

which together with (7.25) implies:

$$\begin{aligned} \Delta_{out} - \Delta_{in} &> \frac{\rho^2 \sigma^2}{4} & \text{if } \gamma_{out} = +1 \\ \Delta_{out} - \Delta_{in} &< \frac{\rho^2 \sigma^2}{4} & \text{if } \gamma_{out} = -1 \end{aligned}$$

Furthermore, defining:

$$\xi \equiv \frac{4(\Delta_{out} - \Delta_{in})}{\rho^2 \sigma^2} \quad (7.27)$$

and using (7.15), the following relationship holds:

$$\gamma_{in} | \xi + 1 | - \gamma_{out} | \xi - 1 | = 2 \quad (7.28)$$

Depending on the outer and inner geometry, and given the energy densities both inside and outside the bubble, there will only be a certain range of possible values for the energy density σ on the surface of the bubble consistent with (7.28). We will use this to constrain the value of σ in the various cases addressed in this paper.

References

- [1] W. Israel, *Nuovo Cim. B* **44S10**, 1 (1966) [Erratum-ibid. B **48**, 463 (1967 NUCIA,B44,1.1966)].
- [2] V. A. Berezin, V. A. Kuzmin and I. I. Tkachev, *Phys. Rev. D* **36**, 2919 (1987).
- [3] K. Lake, *Phys. Rev. D* **29** (1984) 1861.
- [4] S. Khakshournia and R. Mansouri, *Phys. Rev. D* **65**, 027302 (2002) [arXiv:gr-qc/0307023].
- [5] A. Vilenkin, *Phys. Rev. D* **27**, 2848 (1983).
- [6] S. W. Hawking and T. Hertog, *Phys. Rev. D* **73**, 123527 (2006) [arXiv:hep-th/0602091].
- [7] S. Kachru, R. Kallosh, A. Linde and S. P. Trivedi, *Phys. Rev. D* **68**, 046005 (2003) [arXiv:hep-th/0301240].
- [8] L. Susskind, arXiv:hep-th/0302219.
- [9] G. W. Gibbons and S. W. Hawking, *Phys. Rev. D* **15**, 2738 (1977).
- [10] S. W. Hawking and I. G. Moss, *Phys. Lett. B* **110**, 35 (1982).
- [11] R. W. Wald, *Phys. Rev. D* **28**, 2118 (1983).
- [12] T. Banks and W. Fischler, arXiv:hep-th/0111142.
- [13] T. Banks and W. Fischler, *Phys. Scripta* **T117**, 56 (2005) [arXiv:hep-th/0310288].
- [14] T. Banks, W. Fischler and L. Mannelli, *Phys. Rev. D* **71**, 123514 (2005) [arXiv:hep-th/0408076].
- [15] D. S. Goldwirth and T. Piran, *Phys. Rept.* **214**, 223 (1992).
- [16] D. S. Goldwirth and T. Piran, *Phys. Rev. Lett.* **64**, 2852 (1990).
- [17] D. S. Goldwirth and T. Piran, *Phys. Rev. D* **40**, 3263 (1989).
- [18] N. Deruelle and D. S. Goldwirth, *Phys. Rev. D* **51**, 1563 (1995) [arXiv:gr-qc/9409056].
- [19] O. Iguchi, H. Ishihara and J. Soda, *Phys. Rev. D* **55**, 3337 (1997) [arXiv:gr-qc/9606012].
- [20] O. Iguchi and H. Ishihara, *Phys. Rev. D* **56**, 3216 (1997) [arXiv:gr-qc/9611047].
- [21] G. Lemaitre, *Gen. Rel. Grav.* **29**, 641 (1997) [*Annales Soc. Sci. Brux. Ser. I Sci. Math. Astron. Phys. A* **53**, 51 (1933)].
- [22] R. C. Tolman, *Proc. Nat. Acad. Sci.* **20**, 169 (1934).
- [23] H. Bondi, *Mon. Not. Roy. Astron. Soc.* **107**, 410 (1947).
- [24] H. Kurki-Suonio, P. Laguna and R. A. Matzner, *Phys. Rev. D* **48**, 3611 (1993) [arXiv:astro-ph/9306009].
- [25] A. Berera and C. Gordon, *Phys. Rev. D* **63**, 063505 (2001) [arXiv:hep-ph/0010280].
- [26] L. F. Abbott, D. Harari and Q. H. Park, *Class. Quant. Grav.* **4**, L201 (1987).
- [27] P. J. E. Peebles, *Astrophys. J.* **147**, 859 (1967).
- [28] S. R. Coleman and F. De Luccia, *Phys. Rev. D* **21**, 3305 (1980).
- [29] E. Farhi and A. H. Guth, *Phys. Lett. B* **183**, 149 (1987).

- [30] E. Farhi, A. H. Guth and J. Guven, Nucl. Phys. B **339**, 417 (1990).
- [31] W. Fischler, D. Morgan and J. Polchinski, Phys. Rev. D **41**, 2638 (1990).
- [32] W. Fischler, D. Morgan and J. Polchinski, Phys. Rev. D **42**, 4042 (1990).
- [33] E. Poisson, “A Relativist’s Toolkit : The Mathematics of Black-hole Mechanics”, Cambridge, UK: Cambridge University Press, 2004
- [34] K. Lake, in *8th Brazilian School of Cosmology and Gravitation*, edited by M. Novello (World Scientific, Singapore, 1988), pp. 1-82.
- [35] P. Laguna-Castillo and R. A. Matzner, Phys. Rev. D **34**, 2913 (1986).
- [36] C. Barrabes and W. Israel, Phys. Rev. D **43**, 1129 (1991).
- [37] N. D. Birrell and P. C. W. Davies, “Quantum Fields in Curved Space,” Cambridge (1999).